Journal of Inorganic Biochemistry 200 (2019) 110813

Contents lists available at ScienceDirect

Journal of Inorganic Biochemistry

journal homepage: www.elsevier.com/locate/jinorgbio

Addition of sodium ascorbate to extend the shelf-life of tuna meat fish: A risk or a benefit for consumers?

Barry D. Howes[a], Lisa Milazzo[a], Enrica Droghetti[a], Mila Nocentini[b,*], Giulietta Smulevich[a,**]

[a] Dipartimento di Chimica "Ugo Schiff", Università di Firenze, Via della Lastruccia 3-13, I-50019 Sesto Fiorentino, (FI), Italy
[b] Istituto Zooprofilattico Sperimentale delle Regioni Lazio e Toscana, Dipartimento di Firenze, Via di Castelpulci 41, I-50010 San Martino alla Palma, (FI), Italy

ARTICLE INFO

Keywords:
Tuna myoglobin
Horse heart myoglobin
Additives
Resonance Raman
Conformational changes

ABSTRACT

We investigate the effects of antimicrobial (sodium citrate tribasic, E331) and antioxidant (ascorbic acid, E300 and sodium ascorbate, E301) additives on the meat drip from defrosted yellowfin tuna fish loins obtained from the local market and horse heart myoglobin. The effects have been followed by electronic absorption, its second derivative spectra, and resonance Raman spectroscopies. Upon addition of the additives, a final form is reached after about 24 h. It is characterized by a 4 nm red-shifted Soret band compared to that typical of the oxy species (418 nm) but with similar Q bands. Resonance Raman experiments carried out in $^{16}O_2$ and $^{18}O_2$ allowed us to identify the presence of the native oxy form coexisting with a second oxygen bound species, characterized by a $\nu(Fe-O_2)$ stretching frequency upshifted 7 cm^{-1} compared to the native oxy form and with a greater (33 cm^{-1}) isotopic shift in $^{18}O_2$. These data suggest the presence of a highly bent ligand conformation. The new species induced by the addition of the additives imparts a red colour to the tuna fish meat, a characteristic that is of some concern. In fact, the presence of the new red form can mask the aging of the product that, consequently, might contain histamine. Furthermore, the electronic absorption spectrum is very similar to that of the tuna fish myoglobin carbon monoxide complex, which has important regulatory consequences. Carbon monoxide treatment of tuna is banned in the EU for masking the effects of aging on the appearance of meats.

1. Introduction

A change of surface colour and the development of a rancid off-odour are the most important phenomena that occur in muscle products during processing and subsequent storage [1]. In fish meat, n-3 polyunsaturated fatty acids (PUFAs) are easily oxidized to form hydroperoxide that, in turn, is readily decomposed to produce a variety of volatile compounds, including aldehydes, ketones and alcohols [2], which are responsible for the undesirable odour of fish muscle [3]. On the contrary, the red colour of tuna flesh is primarily due to the presence of relatively large amounts of the ferrous myoglobin oxygen complex (oxy-Mb). This derivative degrades during storage, ultimately forming the brown oxidized form of the protein (met-Mb) [4,5]. The reaction products of lipid oxidation compromise further the meat colour by accelerating Mb oxidation [6].

Colour is a prime sensory parameter that determines consumer acceptance of a meat product and in particular the bright red colour of tuna muscle is an economically important factor as consumers consider the red muscle colour to be an indicator of freshness [7,8]. Therefore, market pressure has led to the implementation of a shelf-life for fish products, during which the nutritional and sensory characteristics do not change. A number of different methods have been used to achieve this goal, which range from freezing and frozen storage to the use of chemical substances for preserving foodstuffs [9]. However, during frozen storage, enzymatic and non-enzymatic rancidity is known to strongly influence the shelf-life of marine products [10,11]. Therefore, many strategies have been developed to inhibit lipid oxidation, not only to minimize rancidity but also to improve colour stability [12]. In general, additives that improve food preservation by countering damage and deterioration caused by chemical reactions (non-enzymatic oxidation, degradation of vitamins and amino acids, etc.), biological (enzymatic oxidation and other degradation mechanisms) and microbiological processes are commonly used. Moreover, carbon monoxide treatment has been used to preserve the red colour typical of fresh meat. This procedure has been mainly applied to tuna, but similar fish such as mahi-mahi and tilapia have also been similarly treated [13]. It results in the formation of the bright cherry red colour characteristic of carboxy-Mb (CO-Mb) complexes, which is stable during frozen storage

* Correspondence to: M. Nocentini, Sharda Cropchem Ltd., Prime Business Park, Dashrathlal Joshi Road, Vile Parle (West), Mumbai 400056, India.
** Corresponding author.
E-mail addresses: m.nocentini@shardaintl.com (M. Nocentini), giulietta.smulevich@unifi.it (G. Smulevich).

https://doi.org/10.1016/j.jinorgbio.2019.110813
Received 18 April 2019; Received in revised form 30 July 2019; Accepted 25 August 2019
Available online 26 August 2019
0162-0134/

and can last beyond the real shelf-life of the fish. Therefore, as a change in colour is used by many consumers as a primary means to assess meat quality, carbon monoxide treatment has the potential to make inferior quality fish appear aesthetically more pleasing to consumers or to mask decomposition resulting in an increased risk of histamine poisoning. In fact, for histidine-rich fishes, such as tuna, mackerel, sardine, herring and swordfish, the fraudulent use of CO determines an significant risk since histamine (oxidative decarboxylation of histidine), responsible for toxicological effects, can be formed [14]. Importantly, carbon monoxide treatment of tuna is banned in the EU for masking the effects of aging on the appearance of meats. Recently, additives like citric acid, ascorbic acid and their salts have been used to prevent oxidation in fish. Citric acid and its salts are widely known for their role as chelators and acidulants in biological systems, inhibiting microbial growth [15]. In regard to the inhibition of lipid oxidation, citric acid has been shown to play a synergic role with primary antioxidants during minced fish processing [16]. In the same way, ascorbic acid (E300) and sodium ascorbate (E301) are commonly used in the preparation of food products to prevent the oxidation of food (colour change of fresh-cut or peeled products) and, therefore, to maintain colour. It has been shown that the rate of lipid oxidation of ordinary skipjack tuna muscle is closely related to ferric Mb formation, and that the addition of antioxidants to fish meat inhibits lipid oxidation as well as myoglobin oxidation in post-mortem meat [17]. Nevertheless, in the last few years (2016–2018), many alerts have been published on the portal of the Rapid Alert System for Food and Feed (RASFF) of the European Commission (https://webgate.ec.europa.eu/rasff-window/portal/) regarding the presence of histamine in thawed yellowfin tuna fillets and tuna slices.

The aim of this study is to investigate the effects of addition of different additives to Mb from tuna fish (TFMb) and horse heart (HHMb). The spectral variations observed in the electronic absorption spectrum upon addition of additives to HHMb, either as a 10% mixture of preservatives [antimicrobial (sodium citrate tribasic, E331) and antioxidant (ascorbic acid, E300 and sodium ascorbate, E301)] or Na ascorbate (or acid ascorbic) as single components of the mixture, give rise to a final form that is very similar to that observed for TFMb. Resonance Raman (RR) experiments carried out in $^{16}O_2$ and $^{18}O_2$ allowed us to identify the presence in the final form of the native oxy form of HHMb coexisting with a second oxygen bound species, with an altered Fe—O_2 bond, as a consequence of a conformational change induced by the presence of the additive. The properties of the latter form display a number of variations compared to the native oxy form of HHMb, being characterized by a ν(Fe—O_2) stretching frequency upshifted by 7 cm^{-1}, a greater (33 cm^{-1}) isotopic shift in $^{18}O_2$ and a 5 nm red shift of the Soret band. These results clearly highlight the presence of a new heme form characterized by a bright colour that masks the aging of the product which, consequently, might contain histamine.

2. Materials and methods

2.1. Materials

HHMb (met form) (purity 95–100%) was purchased from Sigma–Aldrich (St Louis, MO). Solutions were prepared in ultra-pure deionised water obtained using a Milli-Q system (Millipore, Milan, Italy) with a resistivity of 18.2 MΩ cm.

Ascorbic acid (E 300), sodium ascorbate (E301), sodium citrate tribasic (E331), and sodium dithionite, were obtained from FlukaChemie (Buchs, Switzerland); KH_2PO_4 and Na_2HPO_4-H_2O, were purchased from Merck (KGaA, Darmstadt, Germany). All experiments were carried out in 0.1 M phosphate buffer, pH 7. All chemicals were of analytical or reagent grade and were used without further purification.

2.2. Sample preparation

The meat drip from defrosted yellowfin tuna loins (*Thunnus albacares*) was collected by using a gastight syringe, placed in a 1-cm path-length quartz cuvette and then diluted to 2 mL with deoxygenated 100 mM phosphate buffer pH 7.0.

The samples of tuna meat drip, from defrosted yellowfin tuna loins in the presence of a mixture of additives were prepared by treating the ferric buffered meat drip (containing TFMb) with the mixture of additives [ascorbic acid E300 (25%), sodium ascorbate E301 (35%), sodium citrate tribasic E331 (30%), NaCl (10%)] to a final concentration corresponding to 10% of weight, similar to that reported by [18].

Samples of HHMb in the presence of additives were prepared by treating 2 mL ferric buffered solutions in a 1-cm path-length quartz cuvette for electronic absorption experiments with the additives to the final following concentrations in weight: Na ascorbate 5% and 10%, ascorbic acid 5% and 10%, sodium citrate tribasic 10% and a mixture of additives 10%. The corresponding samples for RR experiments were prepared by treating 100 μL ferric solutions in a 5-mm NMR tube.

Ferrous samples at pH 7.0 were prepared by addition of a freshly prepared sodium dithionite solution (15 mg/mL) to the ferric forms previously flushed with nitrogen. The Fe(II)-CO complex at pH 7.0 was prepared by flushing the ferric sample firstly with nitrogen, then with CO (Rivoira, Milan, Italy), and reducing the heme by addition of a freshly prepared sodium dithionite solution (15 mg/mL).

The Fe(II)-$^{16}O_2$ complex of HHMb at pH 7.0 was prepared by reduction of the ferric form with a freshly prepared sodium dithionite solution (15 mg/mL), followed by gel filtration on a Sephadex G-25 Medium column equilibrated with phosphate buffer.

The Fe(II)-$^{18}O_2$ complex of HHMb at pH 7.0 was prepared by flushing the ferric sample firstly with nitrogen and then with $^{18}O_2$ (97 atom % $^{18}O_2$, Sigma-Aldrich, St. Louis, MO, U.S.A.), and reducing the heme by addition of a freshly prepared sodium dithionite solution (15 mg/mL).

The $^{18}O_2$ complex of HHMb + 5% Na ascorbate at pH 7.0 was prepared by flushing the admixture firstly with nitrogen and then with $^{18}O_2$ (97 atom % ^{18}O, Sigma-Aldrich, St. Louis, MO, U.S.A.).

HHMb protein concentrations of ca. 6 and 20 μM were used for the electronic absorption and RR samples, respectively. The protein concentration was determined on the basis of the molar absorptivity (ε) of 188 mM^{-1} cm^{-1} at 409 nm for the ferric protein [19].

2.3. Methods

Electronic absorption spectra, measured with a Cary 60 (Agilent Technologies, Glostrup, Denmark) at 25 °C, were recorded using a 1-cm cuvette and a 600 nm/min scan rate. Absorption spectra (using a 5-mm NMR tube and 300 nm/min scan rate) were measured both prior to and after RR measurements to ensure that no degradation had taken place under the experimental conditions used.

The RR spectra were obtained at 25 °C using a 5-mm NMR tube by excitation with the 413.1 nm line of a Kr^+ laser (Innova 300C, Coherent, Santa Clara, CA, USA). Backscattered light from a slowly rotating NMR tube was collected and focused into a triple spectrometer (consisting of two Acton Research SpectraPro 2300i and a SpectraPro 2500i in the final stage with a 1800 grooves/mm grating) working in the subtractive mode, equipped with a liquid nitrogen-cooled CCD detector. A spectral resolution of 4 cm^{-1} and spectral dispersion of 1.2 cm^{-1}/pixel were calculated theoretically on the basis of the optical properties of the spectrometer for the 1800 grooves/mm grating.

A cylindrical lens, which focuses the laser beam in the sample to a narrow strip rather than the usual point, was used to collect the spectra of the ferric and ferrous-CO samples in the presence of 5% Na ascorbate, due to its tendency to photolyse under irradiation. As a consequence of the sample sensitivity to laser induced photolysis, the RR spectra were carefully monitored at 5 min intervals and samples

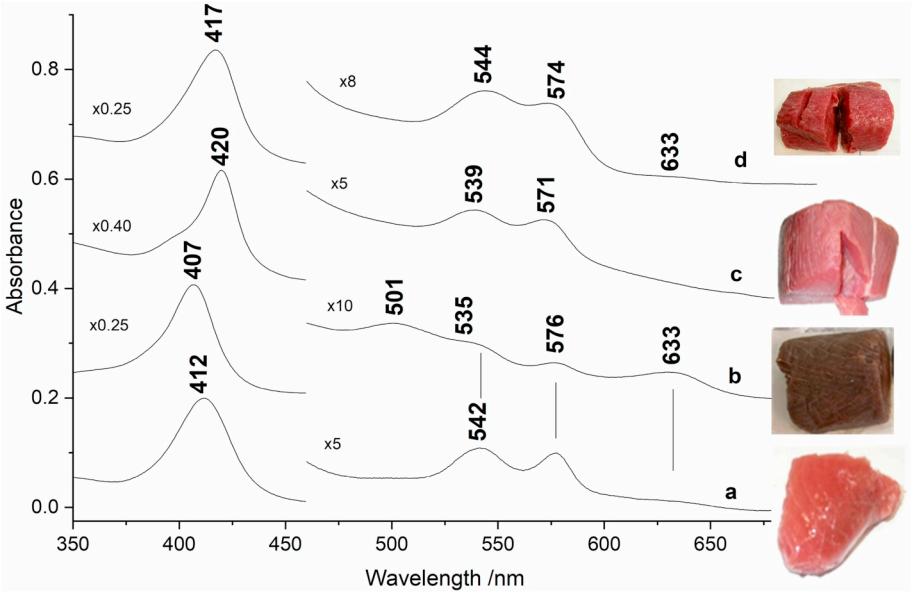

Fig. 1. Electronic absorption spectra of defrosted yellowfin tuna fish meat drip in 100 mM phosphate, pH 7: a) untreated fresh sample obtained from an Italian market; b) untreated aged sample; c) treated with CO and d) sample obtained from an Italian market treated with ascorbic acid (E300), sodium ascorbate (E301) and sodium citrate tribasic (E331), as reported on the product label. Images of the corresponding tuna fish fillets are also shown.

changed every 30 min.

The RR spectra were calibrated with indene and carbon tetrachloride as standards to an accuracy of 1 cm^{-1} for intense isolated bands. All RR measurements were repeated several times under the same conditions to ensure reproducibility. To improve the signal-to-noise ratio, a number of spectra were accumulated and summed only if no spectral differences were noted. All spectra were baseline-corrected. A spectral simulation program (LabCalc, Galactic Industries) using a Lorentzian or Gaussian line shape was used to determine the peak positions, bandwidth, and intensity. The frequencies of the bands were optimized to an accuracy of 1 cm^{-1} and the bandwidths to an accuracy of 0.5 cm^{-1}.

3. Results and discussion

3.1. Electronic absorption spectra

3.1.1. Tuna Mb

The images of four different yellowfin tuna fish fillets together with the electronic absorption spectra of the corresponding meat drip are shown in Fig. 1. The colour of the meat changes dramatically from (a) fresh, (b) aged, (c) CO-treated, and (d) treated with a mixture of ascorbic acid (E300), sodium ascorbate (E301) and sodium citrate tribasic (E331). Accordingly, the corresponding electronic absorption spectra display distinct differences. In fact, the heme active site of myoglobin gives rise to strong electronic transitions at about 400 nm (Soret or B band) and 500–580 nm (Q bands), with the wavelength maxima being dependent on the oxidation, spin, and coordination states of the heme iron. The spectra of oxy-myoglobin, deoxy-myoglobin, met-myoglobin and CO-myoglobin can be distinguished by their peak positions and relative intensities [20] and become very distinct in the second derivative absorption spectra [21].

The fresh sample (a) gives rise to a Soret maximum at 412 nm and Q bands at 542 and 576 nm, due mainly to the oxy-TFMb complex. However, the 2 nm Soret blue-shift compared to a pure oxy-TFMb sample [21], together with the presence of a CT1 band at 633 nm, indicates also the presence of a small amount of oxidized ferric TFMb. The aged sample (b) is characterized by maxima at 407, 501 and 540 nm, and 633 nm, due to the oxidation of ferrous oxy-TFMb to the met-TFMb state, whereas the CO-treated sample (c) shows maxima at 420, 539 and 571 nm, similar to those reported previously for the TFMb-CO complex [21]. The UV–Vis spectrum of fresh tuna fillet in the presence of the mixture of preservatives (d), characterized by maxima at 417, 544 and 574 nm, is in between those of the oxy-TFMb and CO-treated samples.

In order to gain insight into the nature of the complex formed in the presence of additives (spectrum d), we undertook an electronic absorption spectroscopic study adding a 10% mixture of additives to the meat drip from defrosted yellowfin tuna fish loins obtained from the local market and diluted in deoxygenated phosphate buffer.

The electronic absorption and second derivative spectra of tuna meat drip diluted in deoxygenated phosphate buffer 30 min, 4 h, and 24 h after the addition of a mixture of additives are shown in Fig. 2A. As noted for the corresponding spectrum in Fig. 1 (trace a), the spectrum of the meat drip alone is mainly characteristic of a mixture of oxy-TFMb and met-TFMb, clearly revealed in the second derivative spectra by Soret bands at 418 nm and 409 nm, respectively [20]. After addition of the mixture of additives, progressive time dependent spectral changes are observed. After 30 min the Soret band at 409 nm red-shifts to 414 nm and the Q-bands at 540 and 577 nm of the oxy form increase, whereas the ferric CT1 band at 633 nm disappears, indicating reduction of the ferric TFMb and complete formation of the oxy-TFMb complex. However, after 4 h, a further red-shift to 421 nm is observed. Although the spectrum does not markedly change further with time, after 24 h a general decrease of the absorbance together with a broadening of the Soret band are observed due to the formation of a small amount of deoxy-TFMb, characterized by a maximum at 431 nm (437 nm in the second derivative spectrum).

The corresponding spectra obtained after reduction with dithionite are reported in Fig. 2B. The reduced untreated meat drip is characteristic of pentacoordinate high-spin (5cHS) deoxy-TFMb with Soret maximum at 431 nm (435/437 nm in the second derivative spectrum), as expected. However, the spectra in the presence of the additives are markedly different. After 30 min a maximum at 421 nm is clearly present, it increases with time at the expense of the 431 nm band. These variations are particularly clear in the second derivative spectra. The final spectrum is characterized by bands at 421, 540 and 568 nm, identical to that obtained without dithionite. This confirms that the preservatives reduce the heme iron and a new species is formed, which is stable after the addition of dithionite.

3.1.2. HHMb

To clarify the nature of the interaction of tuna Mb with the additives and identify the ligand which binds TFMb in the final form, the effects of the additives [Na ascorbate (5% & 10%), ascorbic acid (5% & 10%),

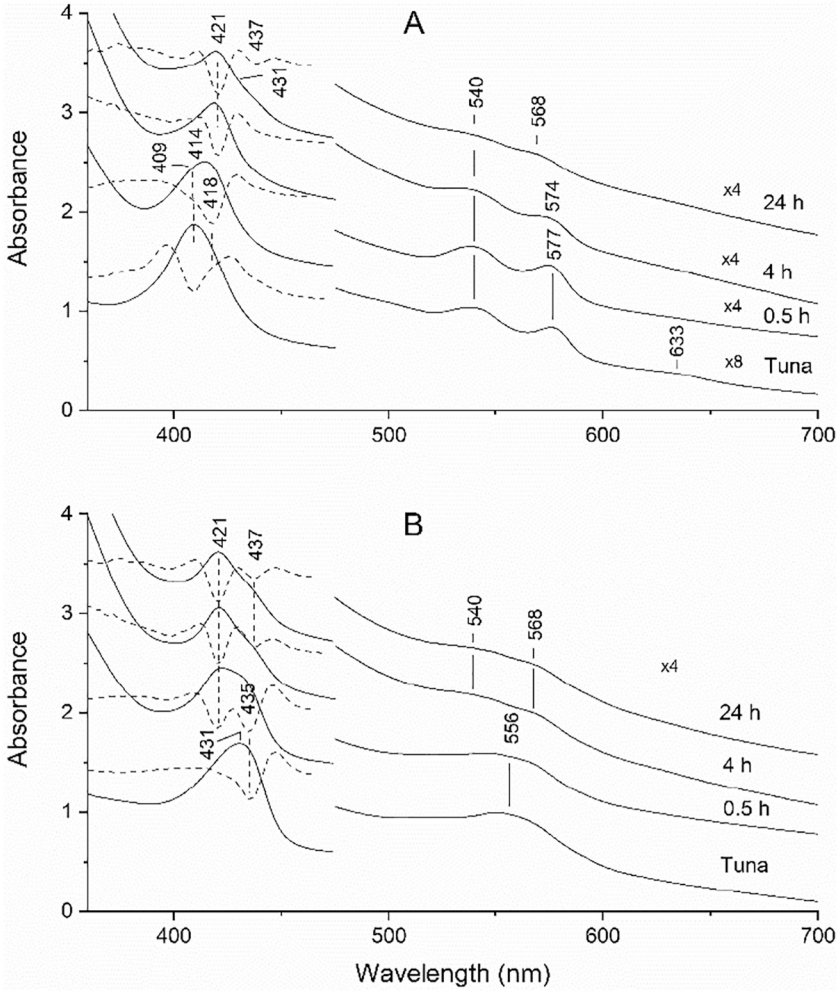

Fig. 2. Electronic absorption and second derivative (dashed line) spectra of defrosted yellowfin tuna fish meat drip in deoxygenated 100 mM phosphate, pH 7 at the times indicated after addition of a 10% mixture of additives (panel A) and the corresponding spectra of the reduced forms (panel B). The 475–700 nm region has been expanded as shown for each spectrum.

sodium citrate tribasic (10%), mixture of additives (10%)] on purified horse heart Mb, have been monitored by following the time course of the UV–vis spectral variations.

It is noted that a comparison of the electronic absorption spectrum of HHMb with that after addition of sodium citrate tribasic (10%) revealed that this additive does not give rise to spectral variations (Fig. S1).

Fig. 3 reports the case of 5% Na ascorbate. Spectral variations are observed immediately after addition of the additive, characterized by the appearance of weak bands at 543 and 581 mn (Fig. 3A). The bands characteristic of ferric HHMb (409, 504 and 633 nm) undergo progressive time dependent changes. The Soret band at 409 nm gradually red shifts and the intensity of the bands at 504 and 633 nm decreases. The presence of isosbestic points at 416, 475, 525 and 595 nm for the spectra 1 to 7 suggests the transition of the hexa-coordinate high spin (6cHS) ferric aquo-HHMb form into a 6c low spin (LS) state in this time period. In fact, the new Q-bands at 543 and 581 nm, typical of a ferrous LS species, progressively increase reaching their maximum intensity after 70 min with a corresponding Soret band at 418 nm (spectrum 7, red). This species is assigned to the ferrous oxy-HHMb form [22,23].

Subsequently, the bands at 543 and 581 nm progressively lose intensity until the final stable spectral form (spectrum 10, blue) is obtained after ca. 21 h (Fig. 3B). The loss of intensity is possibly related to the formation of a second ferrous LS species with different (lower) extinction coefficient. The final spectral form is characterized by a narrow Soret at 422 nm, Q bands at 543 and 581 nm, and the complete loss of the characteristic bands of ferric HHMb. The absence of isosbestic points for the spectra recorded after 70 min is consistent with the formation and significant increase of the aforementioned second ferrous LS species, which characterizes the final form and differs from that typical of oxy-HHMb.

In conclusion, the final form shows a 4 nm red-shift of the Soret band compared to that typical of the HHMb oxy species (418 nm) but with similar Q bands. Hence, the electronic absorption spectrum suggests the presence of an oxy-HHMb form different from that normally observed. This is possibly due to a conformational variation of the heme cavity induced by the additives characterized by an altered $Fe—O_2$ bond.

It should be noted that various preparations of HHMb + 5% Na ascorbate demonstrated that the evolution of the time course displays some variability. In particular, although for some preparations the formation of a deoxy-HHMb species is not observed, as for the case presented in Fig. 3, for other preparations a deoxy-HHMb species is clearly observed at approximately 5 h after the addition of ascorbate, which remains as a minor species for a variable time interval before disappearing. In fact, it is completely absent in the final form. A possible explanation of this anomalous behaviour is that it is correlated with slight differences in the concentration of the reducing agent. In fact, a higher reductant concentration could lead to the rupture of the $Fe—O_2$ bond and, consequently, the formation of the deoxy-HHMb

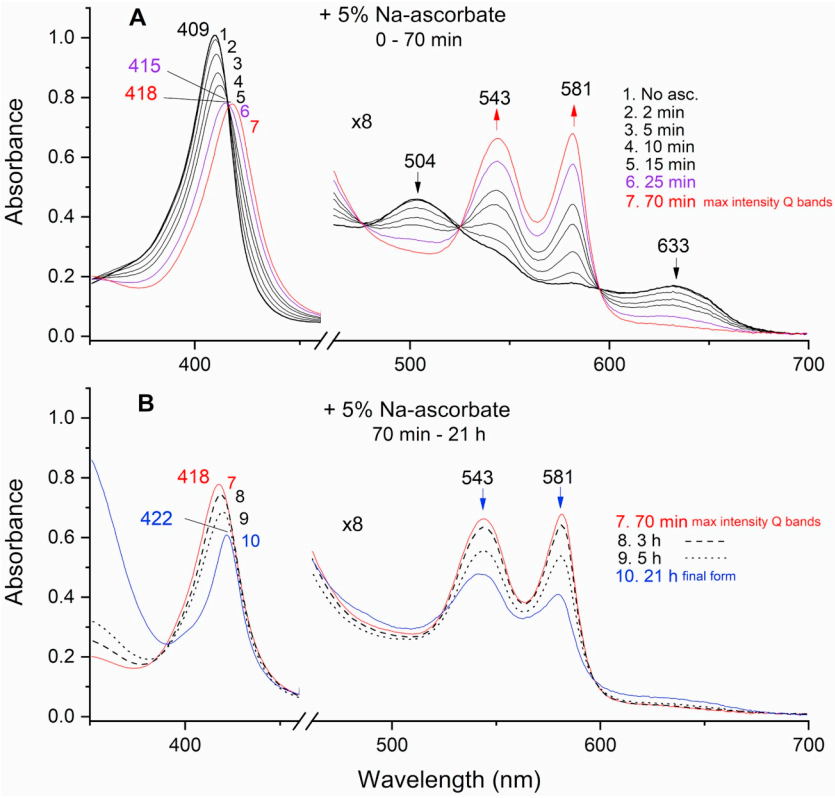

Fig. 3. Time course of the effects on the electronic absorption spectra of 5% Na ascorbate (final concentration of Na ascorbate 26 mM) addition to HHMb in 100 mM phosphate, pH 7. Panel A, variations observed in the time period 0–70 min (spectra 1–7); Panel B, variations observed in the time period 70 min–21 h (spectra 7–10). The arrows indicate the decrease of the ferric HHMb bands (black), the increase of bands at 543 and 581 nm (red), and the subsequent decrease of these bands (blue). (For interpretation of the references to colour in this figure, the reader is referred to the web version of this article.)

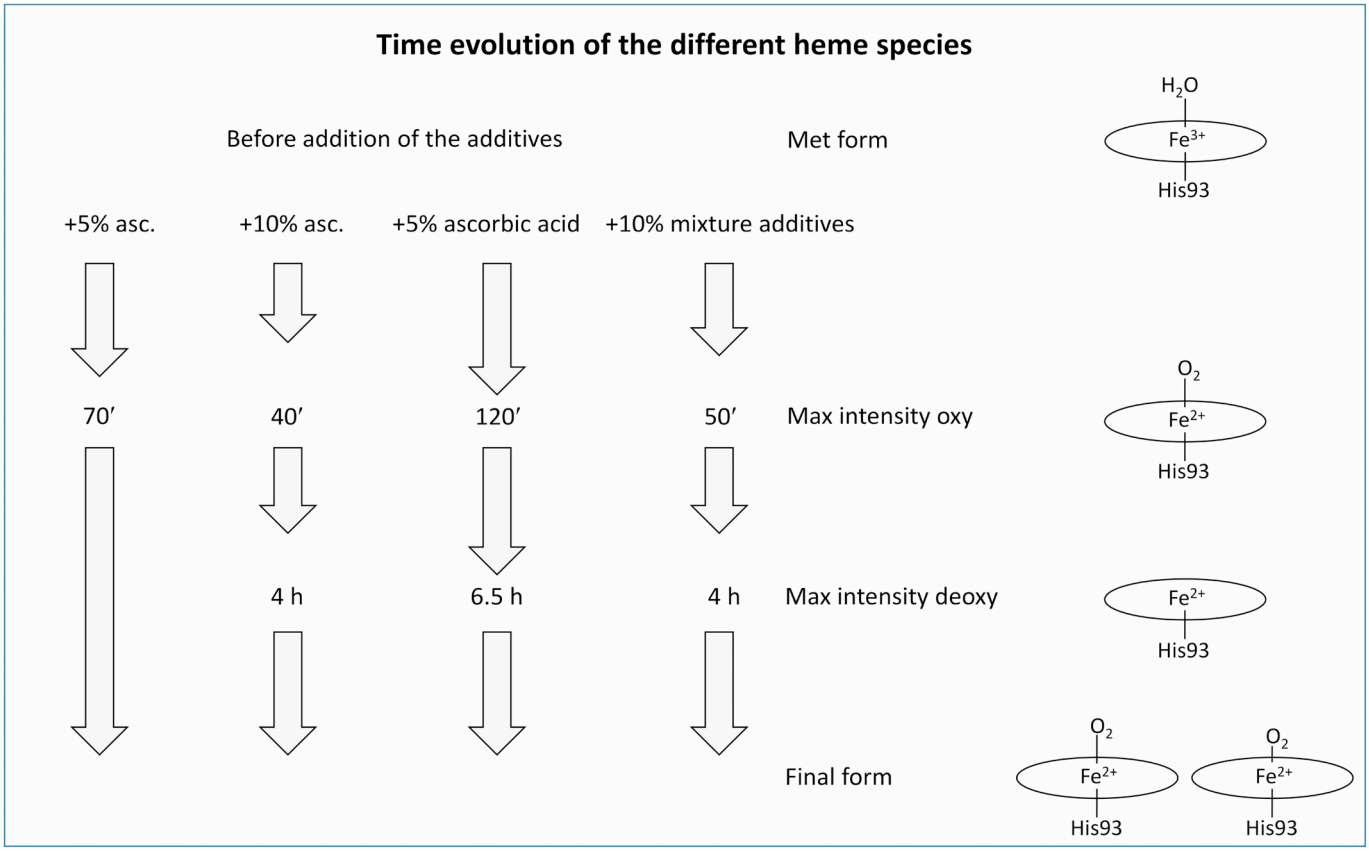

Scheme 1. Schematic representations of the time evolution (left) and of the heme coordination (right) of the different species that form upon addition of the various additives. The final form, completely formed after 20 + h, is constituted by two oxygen bound species. One corresponds to that of the oxy complex, whereas in the second species a conformational variation of the heme cavity induced by Na ascorbate strengthens the Fe—O_2 bond.

species. However, it is also possible that the presence/absence of the deoxy form may be correlated to a lower/greater level of oxygen in solution.

Selected second derivative absorption spectra (Fig. S2) of the time course presented in Fig. 3 reveal additional aspects. In particular, the Soret band of the initial (411 nm) and final (422 nm) spectra are symmetric and narrow indicating that they correspond to pure species. An isosbestic point is again observed at 415 nm for spectra in the time interval 0–70 min; after 70 min (corresponding to the maximum intensity of the Q-bands and the oxy-HHMb form at 419 nm), the Soret slowly red-shifts to its final form (Soret 422 nm) after ca. 21 h.

Hence, the time dependent variations of the electronic absorption spectrum can be summarised as follows. As expected, the ferric form is reduced by the presence of the additives forming, in the presence of atmospheric oxygen, the oxy-HHMb species (Soret band at ca. 418 nm and Q-bands at 543, 581 nm). Normally, although not always for the case of 5% Na ascorbate, a small quantity of transient deoxy-HHMb (Soret at ca. 435 nm) is then formed due to the dissociation of O_2 from the heme iron, which remains for a variable time period and is completely absent in the final form. After the oxy species has achieved its maximum population, the final form gradually increases with time at the expense of the oxy form and is characterized by a 6cLS ferrous form with Soret at ca. 422 nm (4 nm red-shifted compared to the oxy form).

Upon increasing the concentration of Na ascorbate to 10% (Fig. S3) a number of differences are observed in the evolution of the time dependent spectral variations; however, the final spectral form after 23 h is identical to that for 5% Na ascorbate. In particular, the reaction time is faster in line with the higher amount of reductant present, as highlighted by the anticipated appearance of the maximum intensity of the oxy-HHMb species LS Q bands (543, 581 nm) and corresponding Soret at 418 nm after 40 min (cf. 70 min for 5% Na ascorbate). The deoxy-HHMb form (shoulder at 435 nm, 439 nm in second derivative) appears after 150 min, reaches its maximum after 4 h and subsequently decreases to be completely absent in the final spectrum after 23 h. In agreement with the case for 5% Na ascorbate, isosbestic points are observed at 416, 480, 525 and 595 nm for the spectra 1–5 (0–40 min) corresponding to the conversion of the ferric form to the oxy-HHMb species. Scheme 1 shows schematic representations of the heme coordination and time evolution of the different species that form upon addition of the various additives.

The spectral variations observed after addition of 5% ascorbic acid (Fig. S4) are similar to those for the case of 5% Na ascorbate. In fact, the final spectrum is very similar with the Soret band at 421 nm. However, the reaction time is slower, as highlighted by the delayed appearance of the maximum intensity of the oxy-HHMb Q bands (543, 581 nm) and corresponding Soret at 417 nm after 120 min (cf. 70 min). Isosbestic points are again observed at 416, 480, 525 and 595 nm for the spectra 1–5 (0–120 min). A minor deoxy species briefly appears after approximately 390 min (shoulder at 435 nm, 439 nm in second derivative), which by 450 min has completely disappeared.

The addition of 10% ascorbic acid causes a significant lowering of the solution pH (pH 5.7), hence, it was not considered further.

The most marked difference of the time course for the 10% mixture of additives (Fig. 4) compared to that for 10% Na ascorbate (Fig. S3) is the slightly slower reaction time. This is highlighted by the delayed appearance of the maximum intensity of the oxy-HHMb Q bands (543, 581 nm) and corresponding Soret at 418 nm after 50 min (cf. 40 min). Interestingly, although slower than for 10% Na ascorbate, it is faster than for 5% Na ascorbate (cf. 70 min) (Fig. 3), consistent with the enhanced presence of reductants (Na ascorbate 3.5%; ascorbic acid 2.5%). All other features of the time dependent spectral variations are very similar in both cases. The deoxy species appears after a similar time interval (4 h) in both cases and has a similar intensity. Once again, the presence of isosbestic points at approximately 416, 480, 525 and 595 nm for spectra 1–4 (0–50 min), suggests the conversion of the ferric 6cHS species into the ferrous oxy-HHMb 6cLS species in this time

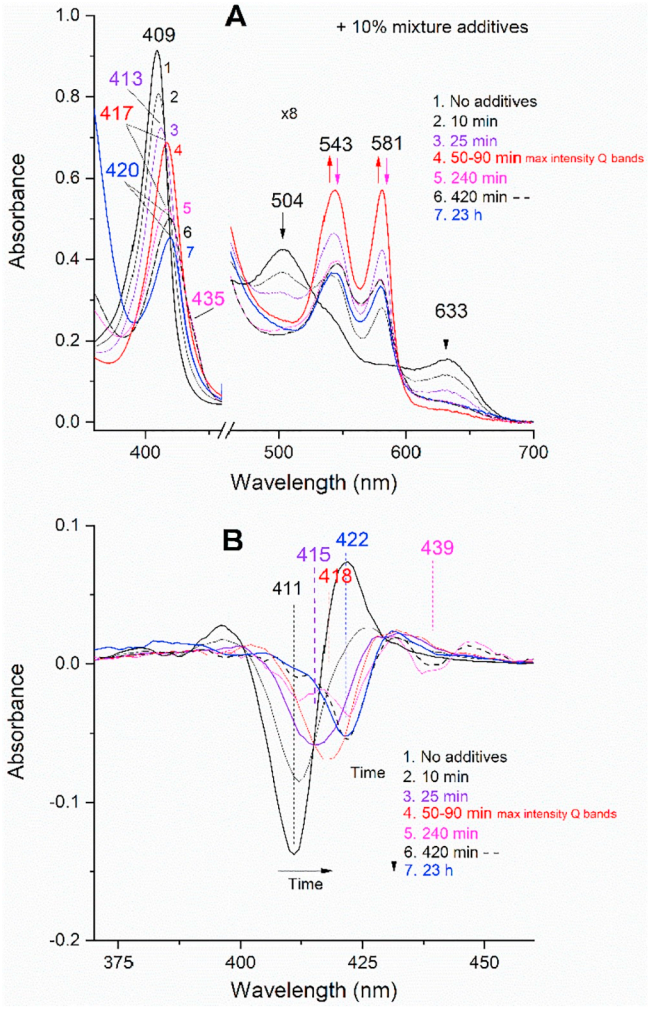

Fig. 4. Effects of the addition of 10% mixture of additives to HHMb in 100 mM phosphate, pH 7. Panel A: Time course of the variations on the electronic absorption spectra (0 − 23 h). The arrows indicate the decrease of the ferric HHMb bands (black), the increase of bands at 543 and 581 nm (red, spectra 1–4), the subsequent decrease of these bands upon formation of the final form (blue, spectra 5–7); Panel B: corresponding second derivative spectra in the Soret region. The arrows indicate the variations of the Soret band with time. (For interpretation of the references to colour in this figure legend, the reader is referred to the web version of this article.)

period. After 23 h the spectrum does not change further. The final spectrum is slightly different compared to that for all other cases [Soret at 420 nm, compared to 421 nm (ascorbic acid) and 422 nm (Na ascorbate)] due to the residual presence of the ferric form at 411 nm (Fig. 4B). In fact, interestingly, in the cases when ascorbic acid is present (5% ascorbic acid and 10% mixture of additives), the spectral contribution due to the residual presence of the ferric HHMb form (band at 411 nm in the second derivative spectra) remains more evident in the second phase of the time course after the oxy species begins to decrease.

3.2. Resonance Raman spectra

To gain further insight into the interaction between TFMb and HHMb and the additives; in particular, to clarify the nature of the final form identified by electronic absorption spectroscopy at the end of the time course, this species was studied by resonance Raman (RR) spectroscopy. The RR technique has been extensively applied over the past several decades to study the structure, function, folding and dynamics

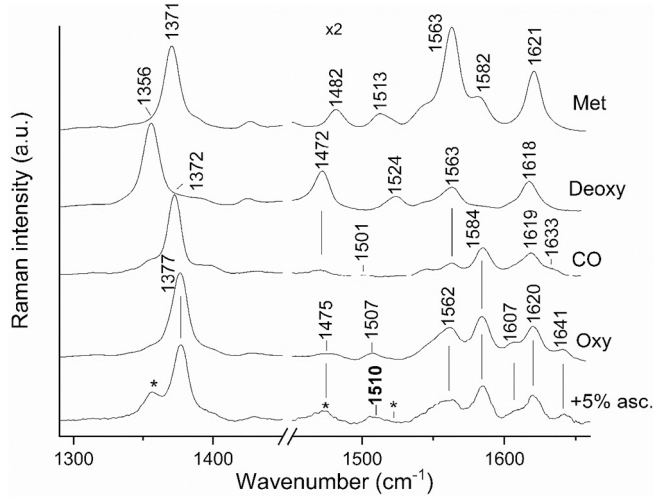

Fig. 5. RR spectra of HHMb + 5% Na ascorbate prepared in NMR tube (100 μL) after 20 h from Na ascorbate addition compared with reference spectra of the met and deoxy forms of HHMb and its complexes with O_2 and CO in the high frequency region. RR experimental conditions: excitation wavelength of 413.1 nm; 1800 grooves/mm grating; (+5% asc), laser power at the sample 1 mW, average of 30 spectra with 150 min integration time; (oxy), laser power at the sample 2 mW, average of 12 spectra with 60 min integration time; (CO), laser power at the sample 0.6 mW, average of 12 spectra with 60 min integration time; (deoxy and met), laser power at the sample 5 mW, average of 6 spectra with 60 min integration time (deoxy), and average of 3 spectra with 30 min integration time (met). The band at 1510 cm^{-1} (bold) identifies a ν_3 band of the HHMb + 5% ascorbate sample. Asterisks indicate bands of the deoxy species. The RR intensities are normalized to that of the ν_4 band. The frequency region 1450–1670 cm^{-1} has been expanded two-fold.

of heme-containing proteins and has been proven exceptionally fruitful. In the context of the present study, it is able to give detailed information not only on the oxidation state of the different species but also identify the nature of the heme bound ligands [24–26].

As the final form is very similar for both tuna fish and horse heart Mb, for all cases studied, the effects of Na ascorbate (5%) on HHMb was chosen for the RR study as it gave rise to the simplest time dependent behaviour.

Fig. 5 compares the RR spectra of HHMb +5% Na ascorbate, 20 h after the addition of Na ascorbate, with reference spectra of the met and deoxy forms of HHMb and its complexes with O_2 and CO. The corresponding electronic absorption spectra are reported in Fig. S5.

The core-size bands at 1562, 1584, 1620 and 1641 cm^{-1} of the HHMb +5% Na ascorbate sample are very similar to those of the oxy spectrum and consistent with the expected LS ferrous heme [27]. The band at 1510 cm^{-1} is assigned to the ν_3 mode, the wavenumber of which is 3 cm^{-1} higher than that observed for the oxy complex of HHMb. It is noted that different preparations of the 5% Na ascorbate sample showed a variable tendency to form the deoxy species, both before and after RR. The Na ascorbate sample shown in Fig. 5 displayed ca. 30% photolysed (deoxy) form, identified by asterisks in the figure. The reference spectra (met and oxy) and (CO and deoxy) are similar to those previously reported [27,28], respectively. It must be noted that the weak 1356 cm^{-1} shoulder on the 1372 cm^{-1} ν_4 band of the CO adduct indicates a low level of photolysis; however, as previously noted for cytochrome *c* peroxidase [29] and for the CO-HHMb adduct [28], the corresponding ν_3 band of the pentacoordinate and photolysed form (1472 cm^{-1}) is more intense than that of the LS CO adduct band at 1501 cm^{-1}.

The corresponding RR spectra in the low frequency region are shown in Fig. 6. This RR region is particularly useful to identify clearly the ferrous LS ligand bound to the heme Fe. In fact, together with the bending vibrations of the porphyrin modes and of the vinyl and propionate substituents [30], bands associated with vibrations of the distal axial ligands have been identified in this region [25]. In particular, in the CO-HHMb adduct the intense band at 509 cm^{-1} is assigned to the ν(Fe—C) mode and the bands at 575 and 581 cm^{-1} to δ(FeCO) and ν_{48}, respectively [28]. The band at 571 cm^{-1} in the oxy-HHMb spectrum is assigned to the ν(Fe—O_2) mode of the oxy complex [27,31]. In the ν(Fe—O_2) region of the HHMb + 5% ascorbate spectrum a broad band at approximately 574 cm^{-1} is clearly observed. Two models are proposed to interpret this broad band based on the curve fitting analysis reported in Fig. S6.

i) Two overlapping ν(Fe—O_2) stretching modes with frequencies at 570 and 578 cm^{-1} (Fig. S6A), highlighting two possible different iron bound species. One of the species (570 cm^{-1}) corresponds to that of the ν(Fe—O_2) mode of the oxy complex, whereas the band at 578 cm^{-1} is proposed to originate from an O_2 bound form in which a conformational variation of the heme cavity, induced by Na ascorbate, alters the Fe—O_2 bond of the oxy form, giving rise to a stronger bond.
ii) Only one ν(Fe—O_2) stretching mode that is inhomogeneously broadened resulting from structural instability of the heme cavity due to interaction with the additive (Fig. S6B), as a consequence of the perturbation of the oxy-heme centre structure induced by Na ascorbate.

The goodness of fit parameters for the two models are the same, hence, they cannot be used to identify a preferred model. However in both cases, the upshifted frequency of the ν(Fe—O_2) stretching mode compared to that of the native oxy-HHMb species is consistent with the 5 nm red shift of the Soret band of HHMb in the presence of 5% ascorbate, (Fig. S5), which indicates the presence of a species in which the O_2 ligand binds more tightly than in the native oxy-HHMb.

The proposed assignment of the bands at 570 cm^{-1} and 578 cm^{-1} (or 573 cm^{-1}, Fig. S6) to ν(Fe—O_2) modes suggests that there should be the corresponding ν(O—O) bands. However, in general, the ν(O—O) mode in oxy-globins (i.e. in adducts with imidazole as proximal axial ligand) is normally not detectable in RR spectra, due to weak enhancement [30]. Nevertheless, RR enhancement of the ν(O—O) mode is observed for imidazole-ligated heme proteins with strong distal H-bonds to the bound O_2 (e.g., *Chlamydomonas* and *Synechocystis* oxyHbs) [32]. The ν(O—O) mode is also detectable in RR spectra when the axial ligand is thiolate; data are available for a number of cysteinyl heme proteins and model complexes [30]. In globins, when observed, the ν(O—O) band is expected at a frequency of ca. 1135 cm^{-1} [31,32]. Comparison of the RR spectra of the Na ascorbate and oxy samples shows that the doublet at ca. 1130 cm^{-1} is very similar for the two cases with the two bands displaying comparable intensity, whereas there is a difference in relative intensity of the two bands for the CO and met samples (Fig. 6). This suggests that for the Na ascorbate and oxy samples there is a ν(O—O) band superimposed on a band of the porphyrin at 1135 cm^{-1}, which is absent in the CO and met samples that gives rise to the relative intensity difference.

To verify that the above-mentioned bands derive from O_2, we studied the Na ascorbate samples with isotopically enriched oxygen ($^{18}O_2$). Comparison of the oxy-HHMb complex in $^{16}O_2$ and $^{18}O_2$ clearly shows that the ν(Fe—O_2) mode band at 571 cm^{-1} shifts to 546 cm^{-1} in $^{18}O_2$ (Fig. 7, Left) and increases in intensity due to overlay with the porphyrin mode at 549 cm^{-1}. The frequency of the ν(Fe—O_2) band in $^{18}O_2$ is determined on the basis of the difference spectrum (546 cm^{-1}, Fig. 8), which has been confirmed by the curve fitting analysis (Fig. S7).

Comparison of the HHMb + 5% ascorbate spectrum in $^{16}O_2$ and $^{18}O_2$ clearly shows that both the 570 and 578 cm^{-1} bands are isotope sensitive, shifting to ca. 548 cm^{-1} in $^{18}O_2$ (Fig. 7, Left). The close similarity of the isotope shift for the $^{18}O_2$ ν(Fe—O_2) bands of oxy-HHMb and HHMb + 5% Na ascorbate is in agreement with their closely similar line shapes which, within the noise level, are very alike (Fig. S8).

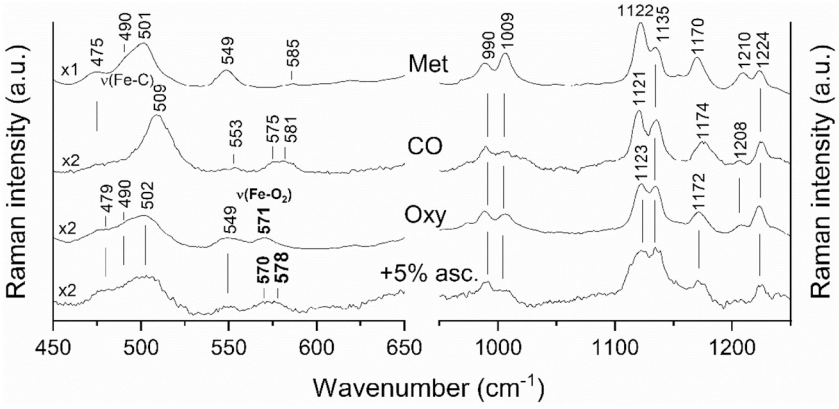

Fig. 6. Low frequency RR spectra of the HHMb + 5% Na ascorbate sample prepared in NMR tube (100 μL), 20 h after Na ascorbate addition, compared with reference spectra of the met form of HHMb and the deoxy-HHMb complexes with O_2 and CO. (Left) low frequency region showing the ν(Fe—O_2) and ν(Fe-CO) bands; (right) intermediate frequency region showing the ν(O—O) band. Experimental conditions as for Fig. 5. Frequencies in bold identify the ν(Fe—O_2) bands of the oxy forms.

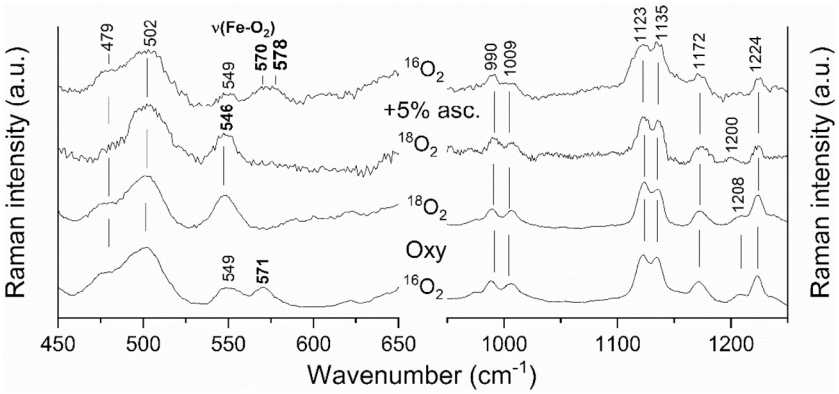

Fig. 7. Comparison of the RR spectra of oxy-HHMb and HHMb + 5%asc in $^{16}O_2$ and $^{18}O_2$ showing the ν(Fe—O_2) (Left) and ν(O—O) (Right) frequency regions. RR experimental conditions: excitation wavelength of 413.1 nm; 1800 grooves/mm grating; (HHMb-$^{16}O_2$)and (HHMb-$^{18}O_2$), laser power at the sample 2 mW, average of 12 spectra with 60 min integration time and of 18 spectra with 90 min integration time, respectively; (+5% asc in $^{18}O_2$) and (+5% asc in $^{16}O_2$) laser power at the sample 1 mW, average of 36 spectra with 180 min integration time and of 16 spectra with 80 min integration time, respectively. The RR intensities are normalized to that of the ν_4 band. Frequencies in bold identify the ν(Fe−O_2) bands of the oxy forms.

This latter observation together with the curve fitting analysis of the oxy-HHMb and HHMb + 5% Na ascorbate spectra in $^{18}O_2$ (Fig. S7) argue in favour of a model in which the broad 574 cm^{-1} band is constituted by two overlapping bands with frequencies at 570 and 578 cm^{-1}. Since the isotope sensitive band at 546 cm^{-1} in $^{18}O_2$ has a typical heme protein line width of 11 cm^{-1}, for both the oxy-HHMb and HHMb +5% Na ascorbate spectra; it would be difficult to reconcile this result with a model in which the corresponding band of the +5% Na ascorbate spectrum in $^{16}O_2$ is inhomogeneously broadened with line width of 20 cm^{-1}.

The frequency region of the ν(O−O) mode is of more difficult analysis. Unfortunately, neither the oxy-HHMb nor HHMb + 5% ascorbate spectrum exhibits any lines that are shifted to lower frequencies by $^{16}O_2$ to $^{18}O_2$ replacement. Instead, in a similar manner as noted above when comparing the spectra in Fig. 7, there is a slight but clear intensity decrease at 1135 cm^{-1} in the $^{18}O_2$ spectra (Fig. 7, Right). Although one possible explanation of this observation may be that for the Na ascorbate and oxy samples there is a ν(O−O) band superimposed on a porphyrin band at 1135 cm^{-1}, this is not confirmed by identification of a corresponding isotopic shift of the band. The calculated shift in $^{18}O_2$ is predicted to be 65 cm^{-1} for the stretching mode of an isolated O−O group. The difference spectra for the oxy-HHMb and HHMb + 5% ascorbate samples display a complicated ensemble of bands that are similar within the noise limits (Fig. 8, Right); however, a negative peak corresponding to an isotope sensitive band in $^{18}O_2$ is not observed, in agreement with the poor enhancement of this mode in these proteins. A similar effect has been reported previously for oxy-myoglobin [33].

The experiment of HHMb + 5% Na in $^{18}O_2$ confirms that the iron ligand of both the species corresponding to the bands observed at 570 and 578 cm^{-1} in the $^{16}O_2$ sample is dioxygen. The two ν(Fe−O_2) stretching modes have significantly different shifts in $^{18}O_2$, of 25 (570 cm^{-1} band) and 33 cm^{-1} (578 cm^{-1} band), respectively; the

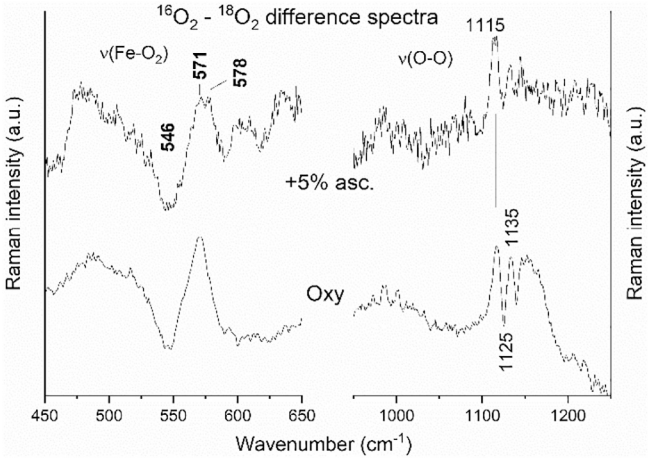

Fig. 8. The $^{16}O_2 - ^{18}O_2$ difference spectra of the RR spectra reported in Fig. 7 showing the ν(Fe—O_2) (left) and ν(O—O) (right) frequency regions.

predicted shift for a Fe−O_2 diatomic oscillator is about 23 cm^{-1}. Interestingly, in heme oxygenase a large isotope shift has been attributed to a highly bent Fe−O−O conformation [34]. The upshifted frequency of the second species is consistent with the 5 nm red shift of the Soret band of the 5% Na ascorbate sample compared to the oxy form, which indicates the presence of a species that binds in a different manner than in the native oxy form. Accordingly, the band at 578 cm^{-1} is proposed to originate from a second oxygen bound species, with an altered (bent) Fe−O_2 bond as a consequence of a conformational change induced by the presence of ascorbate in the heme cavity.

4. Conclusions

The study of the effects of antioxidants on Mb from tuna fish and horse heart clearly indicates that the spectral variations of the electronic absorption spectra induced by addition of either a 10% mixture of preservatives or of Na ascorbate (or ascorbic acid) as single components of the mixture, give rise to a final form which shows very similar UV–Vis spectra for all cases studied, i.e. narrow Soret band at ca. 422 nm, Q-bands at 543 and 581 nm.

On the basis of the electronic absorption spectra the nature of the final form cannot be explicitly determined; however, the RR spectrum of the 5% Na ascorbate sample enables two potentially feasible cases to be unequivocally excluded. First, despite the very close similarity of the UV–vis spectra of the Na ascorbate sample and that of the CO-HHMb complex the heme ligand cannot be CO, as the intense ν(Fe-CO) band is not observed in the low frequency RR spectrum (Fig. 6). A hydroxyl ligand can also be excluded since the low-spin ν(Fe-OH) stretching mode of met HHMb gives rise to a band at 550 cm^{-1} [35], lower than that of the band deriving from the unknown ligand (578 cm^{-1}). Furthermore, the UV–vis spectrum of the final species is typical of a ferrous LS form and very different from that expected for a ferric hydroxyl form.

Nevertheless, the RR spectrum of the 5% Na ascorbate sample is able to offer clear insight into the nature of the final form. In fact, the two RR bands at 570 and 578 cm^{-1} in the low frequency region are of particular interest. On the basis of the isotopic shift observed in $^{18}O_2$, both the 570 and 578 cm^{-1} bands (accidentally) shift to the same frequency (546 cm^{-1}). Therefore, the former band, is due to the $\nu(Fe{-}O_2)$ stretching mode of the oxy form of HHMb, whereas the band at 578 cm^{-1} is proposed to originate from a second oxygen bound species, with an altered $Fe{-}O_2$ bond as a consequence of a conformational change induced by the presence of ascorbate. The present results indicate that even if the additives under study are authorized by the EU (Commission Regulation (EU) No. 1129/2011), they cause changes in the tuna meat which cannot be simply ascribed to natural processes. The new species that is completely formed 24 h after the addition of a mixture of additives imparts a red colour to the tuna fish meat. This characteristic induced by the addition of the additives is of some concern, as the bright red colour of tuna muscle is a prime sensory parameter that determines consumer acceptance of a meat product, the red muscle colour usually being taken as an indicator of freshness. Hence, the presence of the new heme form can mask the aging of the product that, consequently, might contain histamine. Moreover, the electronic absorption spectrum of this form is similar to that of the CO complex (Figs. 1 & 2). Carbon monoxide treatment of tuna is banned in Canada, Japan, Singapore, and labelling is required in the United States. In Europe the use of CO as an additive is also not permitted (Commission Regulation (EU) No. 1129/2011). Consequently, a monitoring program of fish products is in force in the European Community. However, the similarity between the Na ascorbate treated TFMb sample and that of the CO-TFMb renders inapplicable any spectroscopic methodology developed to detect the presence of the illicit use of CO in tuna meat [21,36].

Abbreviations

HHMb	horse heart myoglobin
TFMb	tuna fish myoglobin
CO-Mb	ferrous carboxy-Mb
Oxy-Mb	ferrous Mb oxygen complex
Met-Mb	ferric Mb
Deoxy-Mb	ferrous Mb
5cHS	penta-coordinate high-spin
6cHS	hexa-coordinate high spin
6cLS	hexa-coordinate low spin
RR	resonance Raman

Author contributions

Mila Nocentini, and **Giulietta Smulevich** conceptualization;
Barry D. Howes, **Lisa Milazzo**, **Enrica Droghetti**, **Giulietta** Smulevich data curation;
Barry D. Howes, **Lisa Milazzo**, **Enrica Droghetti** formal analysis;
Mila Nocentini, **Giulietta Smulevich** project administration;
Barry D. Howes, **Lisa Milazzo**, **Mila Nocentini**, **Giulietta Smulevich** writing, review and editing;
Barry D. Howes, **Lisa Milazzo**, **Enrica Droghetti**, **Mila Nocentini**, **Giulietta Smulevich** investigation;
Barry D. Howes, **Lisa Milazzo**, **Enrica Droghetti** methodology;
Mila Nocentini, **Giulietta Smulevich** supervision;
Mila Nocentini, **Giulietta Smulevich**, funding acquisition;
Barry D. Howes, **Giulietta Smulevich** writing-original draft.

Acknowledgements

This work was supported by the Italian Ministry of Health, Rome, Italy (IZSLT 10/15 RC).

Appendix A. Supplementary data

Supplementary data to this article can be found online at https://doi.org/10.1016/j.jinorgbio.2019.110813.

References

[1] C. Faustman, R.G. Cassens, The biochemical basis for discoloration in fresh meat: a review, J. Muscle Foods 1 (1990) 217–243.
[2] I.F.F. Benzie, Lipid peroxidation: a review of causes, consequences, measurement and dietary influences, Int. J. Food Sci. Nutr. 47 (1996) 223–261.
[3] D.B. Josephson, R.C. Lindsay, D.A. Stuiber, Variations in the occurrences of enzymatically derived volatile aroma compounds in salt and freshwater fish, J. Agric. Food Chem. 32 (1984) 1344–1347.
[4] G. Tajima, K. Shikama, Autoxidation of oxymyoglobin. An overall stoichiometry including subsequent side reactions, J. Inorg. Biochem. 262 (1987) 12603–12606.
[5] N.F. Haard, Biochemistry and chemistry of color and color changes in seafoods, in: G.J. Flick, R.E. Martin (Eds.), Advances in Seafood Biochemistry – Composition and Quality, Technomic Publishing Company Inc., Lancester, PA, 1992, pp. 305–360.
[6] C. Faustman, D.C. Liebler, T.D. McClure, Q. Sun, α,β-Unsaturated aldehydes accelerate oxymyoglobin oxidation, J. Agric. Food Chem. 47 (1999) 3140–3144.
[7] R.A. Mancini, M.C. Hunt, Current research in meat color, Meat Sci. 71 (2005) 100–121.
[8] E. Risvik, Sensory properties and preferences, Meat Sci. 36 (1994) 67–77.
[9] M.C. Erickson, Lipid oxidation: flavor and nutritional quality deterioration in frozen foods, in: M.C. Erickson, Y.-C. Hung (Eds.), Quality in Frozen Food, Springer, Boston, MA, 2011, pp. 141–173.
[10] R.J. Hsieh, J.E. Kinsella, Oxidation of polyunsaturated fatty acids: mechanisms, products and inhibition with emphasis on fish, Adv. Food Nutr. Res. 33 (1989) 233–341.
[11] P. Harris, J. Tall, Rancidity in fish, in: J.C. Allen, R.J. Hamilton (Eds.), Rancidity in Foods, Chapman and Hall, London, 1994, pp. 256–272.
[12] C. Faustman, Q. Sun, R.A. Mancini, S.P. Suman, Myoglobin and lipid oxidation interactions: mechanistic bases and control, Meat Sci. 86 (2010) 86–94.
[13] M.O. Balaban, H.G. Kristinsson, B. Welt, Color enhancement and potential fraud in using CO, in: W.S. Otwell, H.G. Kristinsson, M.O. Balaban (Eds.), Modified Atmospheric Processing and Packaging of Fish: Filtered Smokes, Carbon Monoxide, and Reduced Oxygen Packaging, Blackwell Publishing, Ames, Iowa, 2006, pp. 127–140.
[14] D. Djenane, P. Roncales, Carbon monoxide in meat and fish packaging: advantages and limits, Foods 7 (2018) 12.
[15] S. Ponce de León, N. Inoue, H. Shinano, Effect of acetic and citric acids on the growth and activity (VB-N) of Pseudomonas sp. and Moraxella sp, Bulletin of the Faculty of Fisheries Hokkaido University 44 (1993) 80–85.
[16] S.P. Aubourg, F. Pérez-Alonso, J.M. Gallardo, Studies on rancidity inhibition in frozen horse mackerel (*Trachurus trachurus*) by citric and ascorbic acids, European Journal of Lipid Science Technology 106 (2004) 232–240.
[17] J.-H. Sohn, T. Ohshima, Control of lipid oxidation and meat color deterioration in skipjack tuna muscle during ice storage, Fish. Sci. 76 (2010) 703–710.
[18] D. Lad, A. Shivekar, Study on the effects of antioxidants citric acid and ascorbic acid on the quality of surmai, *Scomberomorus guttatus*, steaks during chilled storage, International Journal of Scientific Research 7 (4) (2018) 17–18.
[19] E. Antonini, M. Brunori, Hemoglobin and Myoglobin in Their Interactions with Ligands. North Holland, Amsterdam, (1971).
[20] F. Adar, Electronic absorption spectra of hemes and hemoproteins, in: D. Dolphin (Ed.), The Porphyrins, Physical Chemistry, Part a, vol. III, Academic Press, New

York, 1978, pp. 167–209.
[21] G. Smulevich, E. Droghetti, C. Focardi, M. Coletta, C. Ciaccio, M. Nocentini, A rapid spectroscopic method to detect the fraudulent treatment of tuna fish with carbon monoxide, Food Chem. 101 (2007) 1071–1077.
[22] S. Herold, M. Exner, T. Nauser, Kinetic and mechanistic studies of the NO·-mediated oxidation of oxymyoglobin and oxyhemoglobin, Biochemistry 40 (2001) 3385–3395.
[23] R.M. Barbosa, A.J. Lopes Jesus, R.M. Santosa, C.L. Pereira, C.F. Marques, B.S. Rocha, N.R. Ferreira, A. Ledo, J. Laranjinha, Preparation, standardization and measurement of nitric oxide solutions, Global Journal of Analytical Chemistry 2 (2011) 272–284.
[24] T.G. Spiro, Resonance Raman Spectra of Heme and Metalloproteins, John Wiley & Sons, 1988.
[25] T. Egawa, S.-R. Yeh, Structural and functional properties of hemoglobins from unicellular organisms as revealed by resonance Raman spectroscopy, J. Inorg. Biochem. 99 (2005) 72–96.
[26] G. Smulevich, B.D. Howes, E. Droghetti, Structural and functional properties of heme-containing peroxidases: A resonance Raman perspective for the superfamily of plant, fungal and bacterial peroxidases, in: E. Raven, B. Dunford (Eds.), Heme Peroxidases, Royal Society of Chemistry, 2015, pp. 61–98.
[27] G. Smulevich, A.R. Mantini, M. Paoli, M. Coletta, G. Geraci, Resonance Raman studies of the heme active site of the homodimeric myoglobin from *Nassa mutabilis*: a peculiar case, Biochemistry 34 (1995) 7507–7516.
[28] F. Rwere, P.J. Mak, J.R. Kincaid, Resonance Raman interrogation of the consequences of heme rotational disorder in myoglobin and its ligated derivatives, Biochemistry 47 (2008) 12869–12877.
[29] G. Smulevich, M.A. Miller, S.D. Gosztola, T.G. Spiro, Photodissociable endogenous ligand in alkaline-reduced cytochrome c peroxidase implicates distal protein tension, Biochemistry 28 (1989) 9905–9908.
[30] T.G. Spiro, A.V. Soldatova, Ambidentate H-bonding of NO and O_2 in heme proteins, J. Inorg. Biochem. 115 (2012) 204–210.
[31] S. Hirota, T. Ogura, E.H. Appelman, K. Shinzawa-Itoh, S. Yoshikawa, T. Kitagawa, Observation of a new oxygen-isotope-sensitive Raman band for oxyhemoproteins and its implications in heme pocket structures, J. Am. Chem. Soc. 116 (1994) 10564–10570.
[32] T.K. Das, M. Couture, Y. Ouellet, M. Guertin, D.L. Rousseau, Simultaneous observation of the O—O and Fe—O_2 stretching modes in oxyhemoglobins, Proc. Natl. Acad. Sci. U. S. A. 98 (2001) 479–484.
[33] M. Tsubaki, N.T. Yu, Resonance Raman investigation of dioxygen bonding in oxycobaltmyoglobin and oxycobalthemoglobin: structural implication of splittings of the bound O—O stretching vibration, Proc. Natl. Acad. Sci. U. S. A. 78 (1981) 3581–3585.
[34] S. Takahashi, K. Ishikawa, N. Takeuchi, M. Ikeda-Saito, T. Yoshida, D.L. Rousseau, Oxygen-bound heme—hemeoxygenase complex: evidence for a highly bent structure of the coordinated oxygen, J. Am. Chem. Soc. 117 (1995) 6002–6006.
[35] A. Feis, M.P. Marzocchi, M. Paoli, G. Smulevich, Spin state and axial ligand bonding in the hydroxide complexes of metmyoglobin, methemoglobin, and horseradish peroxidase at room and low temperatures, Biochemistry 33 (1994) 4577–4583.
[36] E. Droghetti, G.L. Bartolucci, C. Focardi, M. Bambagiotti-Alberti, M. Nocentini, G. Smulevich, Development and validation of a quantitative spectrophotometric method to detect the amount of carbon monoxide in treated tuna fish, Food Chem. 128 (2011) 1143–1151.